Research on Output Characteristics of Different PV Array Structures with Partial Shadow

Zhonghua Yun, Jun Jiang

School of Engineering, Tibet University, Lhasa 850012, China

Email：zhonghuayun@utibet.edu.cn

Abstract. Partial shading makes output curve of photovoltaic array non-linear, in this paper, the working characteristics of PV cells were simulated based on the mathematical model of PV cells, the reason and the solution of the thermal spot effect of the photovoltaic array were analysed, the output characteristics of different photovoltaic arrays were deduced and analysed. The simulation results show that in the case of different shadows, the output power of the different array structure is different. We can choose the appropriate PV array structure according to the actual environmental conditions to improve the power generation efficiency.

1. Introduction

In recent years, Photovoltaic (PV) energy has been paid more and more attention for its renewable cleaning advantages. But because the PV cells are vulnerable to the shadow of the environment, they and the PV cells exhibit strong non-linear characteristics under partial shading. In order to study the working characteristics of PV arrays under partial shading, in this paper the working characteristics of PV arrays with different structures under partial shading were analyzed based on the mathematical model of PV cells, the results show that the output characteristics of different array structures are different under partial shadows. Therefore, in practical work, we can choose the optimal array structure according to different environments to improve the efficiency of PV systems.

2. Analysis of Mathematical Model of PV Array

The PV array is composed of PV modules, each module consists of multiple PV cells, the characteristic of the PV cell can be expressed by a diode equivalent model taking into account the avalanche breakdown current I_v, In practice, the manufacturer only gives the open circuit voltage U_{oc}, the short-circuit current I_{sc}, the peak voltage Um and the peak current I_m of the PV module under the standard test conditions, The bipolar diode model for PV cells shown in Fig.1 for taking into account the depletion zone energy loss [1-2]. According to the equivalent circuit model of PV cells and Kirchhoff 's law, the mathematical model of PV cell can be written as Eq.(1)

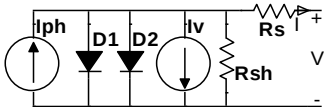

Fig.1 bipolar mathematical model of PV cell

$$I = I_{ph} - I_{D1} - I_{D2} - I_v - I_{sh} \tag{1}$$

The PV module may be exposed to non-uniform irradiation in working condition, that is, in this case the PV module under the shadow of the array may have a negative voltage, because of that, usually the PV module will be connected in parallel with a bypass diode, and when a component produces a negative voltage, the bypass diode will be turned on to protect the PV cell. In this way, the avalanche breakdown current I_v can be ignored when analyzing the operation of the PV cell under

partial shading. The equivalent model with seven parameters is shown in eq. (2) [2-4].

$$\begin{cases} I = I_{ph} - I_{s1}\left[\exp\left(\left(V + IR_s\right)/a_1V_{T1}\right) - 1\right] - I_{s2}\left[\exp\left(\left(V + IR_s\right)/a_2V_{T2}\right) - 1\right] - \left(V + IR_s\right)/R_{sh} \\ V = V_T \ln\left\{\exp\left[-\left(V + IR_s\right)/V_{T2}\right]\left[\left(I_{ph} + I_{s1} + I_{s2} - I\right)/I_{s2} - \left(V + IR_s\right)/\left(R_{sh}I_{s2}\right)\right] - 1\right\} - IR_s \\ V_T = V_{T1}V_{T2}/\left(V_{T1} - V_{T2}\right) \end{cases} \quad (2)$$

In Eq.(2), I_{ph} is photocurrent, I_{s1} and I_{s2} are the currents flowing through the diodes D_1&D_2, R_s is the series resistance, R_{sh} is the parallel resistance, V and I are the output current and the output voltage, a_1, a_2 are the terminal voltage and the ideal coefficient of the two diode ,$V_{T1}=a_1N_skT/q$, $V_{T2}=a_2N_skT/q$ denotes the terminal voltage of the N battery cells connected in series, q is the electron charge (1.60217×10^{-19}C), K is the Boltzmann constant (1.3807×10^{-23}J/K).This equation is more accurate but contains 7 parameters, which is more difficult to calculate, therefore, considering the temperature and irradiance, the equation for the current I_{ph} and the diode saturation current I_s can be written as eq.(3).

$$\begin{cases} I_{ph} = \left(I_{ph,ref} + K_i\Delta T\right)G / G_{ref} \\ I_s = I_{s,ref}\left(T_{ref}/T\right)^3 \exp\left[\left(qE_g/ak\right)\left(1/T_{ref} - 1/T\right)\right] \end{cases} \quad (3)$$

In Eq.(3), $I_{ph,\ ref}$ is the photocurrent in standard environment (25°C, 1000W/m^2), $I_{s,\ ref}$ is the saturation current, G is the actual irradiance, G_{ref} is the standard irradiance, K_i is the short circuit factor provided by the manufacturer, E_g is the bandgap energy of the semiconductor, T_{ref} is the reference temperature, T is the P-N junction temperature, $\Delta T=T-T_{ref}$, the improved saturation current equation considering the temperature can be written as eq.(4), the I_s can written as eq.(5). By the improved algorithm [2], usually the model is the most accurate when $a2\geq1.2$, if $(a_1+a_2)/P = 1$, $a_1 = 1$, the $P\geq2.2$, the I_s can be written as in Eq. (6), the K_v is the open circuit voltage coefficient provided by the manufacturer.

$$I_s = \left(I_{sc,ref} + K_i\Delta T\right)/\left\{\exp\left[\left(V_{oc,ref} + K_v\Delta T\right)/aV_T\right] - 1\right\} \quad (4)$$

$$I_s = \left(I_{sc,ref} + K_i\Delta T\right)/\left\{\exp\left[\left(V_{oc,ref} + K_v\Delta T\right)/\left(\left(a_1 + a_2\right)/P\right)V_T\right] - 1\right\} \quad (5)$$

$$I_{s1} = I_{s2} = \left(I_{sc,ref} + K_i\Delta T\right)/\left\{\exp\left[\left(V_{oc,ref} + K_v\Delta T\right)/V_T\right] - 1\right\} \quad (6)$$

We can calculate the remaining two parameters by using the principle of matching the maximum power point and the measured point parameters, because of $V_{test} = V_{mpp}$, $I_{test} = I_{mpp}$, the two parameters can be written as Eq. (7), the initial conditions of R_{s0} and R_{sh0} are given in the equations.

$$\begin{cases} R_{sh} = \left(V_{mpp,ref} - I_{mpp,ref}R_s\right)/\left\{I_{ph} - I_{s1}\left[\exp\left(\dfrac{V_{mpp,ref} + I_{mpp,ref}R_s}{a_1V_T}\right) - 1\right] - I_{s2}\left[\exp\left(\dfrac{V_{mpp,ref} + I_{mpp,ref}R_s}{a_2V_T}\right) - \dfrac{P_{max,E}}{V_{mpp,ref}}\right]\right\} \\ R_{so} = 0, \quad R_{sho} = V_{mpp,ref}/\left(I_{sc,ref} - I_{mpp,ref}\right) - \left(V_{oc,ref} - V_{mpp,ref}\right)/I_{mpp,ref} \end{cases} \quad (7)$$

So the output current of the PV cell can be calculated using the Newton-Raphson iterative method. Taking BP Solar MSX-60 as an example to model the PV cell using M-function, the parameters are I_{sc}=3.8A, V_{oc}=21.1V, I_{mpp}=3.5A, V_{mpp}=17.1V, R_{sh}=176.4Ω, R_s=0.35Ω, K_v=-80mV/°C, K_i=3mA/°C, $I_{s1}=I_{s2}=4.704\times10^{-10}$A, N_s=36. The characteristics of the modules in different light and temperature of the simulation shows in Fig.2.Which can be seen that the dual diode model is more accurate.

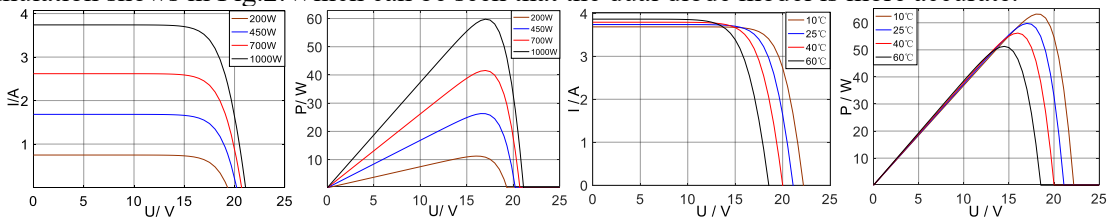

(a) Different light (b) Different temperature

Fig. 2 Output characteristics at different temperatures and light conditions

3. Analysis of hot spot effect

Usually a single PV module output power is small and can't meet the requirements, so a plurality of PV cells can be made into arrays to output larger power. However, PV arrays often encounter various

shadows caused by clouds, shade, birds, etc. At this time, the output current of a PV cell that is blocked is less than the series circuit current, and then the voltage of the blocked battery may be negative and the battery will turn into a load mode, when this happens, the battery may heat up and form hot spots. If we assume that the area of the PV cell is S, the area being blocked is S_{shadow}, the occlusion rate λ and the shadow current $I_{ph,\,shadow}$ can be written as Eq. (8)

It can be seen from Fig.1 that in order to make the PV cell output larger power, we need to decrease the series resistance R_s and increase the parallel resistance R_{sh}. However, the cause of the occurrence of hot spots is the uneven raw materials, the production process quality and the performance matching problems of the battery, etc. The intensity of hot spot is affected by the photocurrent per unit area of PV cell [6-7], the temperature calculation formula of the PV cell at work is shown in Eq.(9), the limit temperature of the PV cell in the reverse bias state can calculated by the Eq.(10)[6-7].

$$\begin{cases} \lambda = S_{shadow} / S \\ I_{ph,shadow} = (1-\lambda) I_{ph} \end{cases} \quad (8)$$

$$T_c = T_a + \alpha G_T (1+\beta T_a)(1-\gamma V_w)(1-1.053\eta_c) \quad (9)$$

$$\begin{cases} T_c \approx T_a + (\alpha - k_G \times 1.053 \times \eta_c) \times G_T + T_h \\ T_h = 0.128 \times J_{sc} \times (n-1) \\ k_G = \alpha \times (1+\beta T_a) \times (1-\gamma V_w) \end{cases} \quad (10)$$

In Eq.(9), T_c is the temperature of the PV cell, T_a is the ambient temperature, α is the temperature coefficient of the PV cell under the sun, G_T is the amount of solar radiation, V_W is the wind speed, η_c is the battery efficiency, and typically the conversion rate of polycrystalline silicon cells is between 15-16%, the conversion efficiency of monocrystalline silicon cells is between 16-18%, and generally β =0.031, γ =0.042. In Eq. (10), J_{sc} is the density of the short-circuit current, typically J_{sc}=35mA/cm^2 in the case of standard test, and n is the length of the battery string.

Because the wind often appears in the daily work, and the wind on the battery can play a cooling effect, usually wind speed is from 0~0.2m/s (level 0) to 56.1~61.2m/s(level 17), consider the wind speed common to work V_W=1.6~3.3m/s (level 2), the battery conversion efficiency η_c =16%, the irradiance is 1000W/m^2, the ambient temperature is 25°C, according to eq.(9) it can be calculated that the battery temperature on working T_c=42.54~43.99°C, it can be seen that the temperature of the battery is inevitably rising at work. And the limit temperature can reached to 115°C in the series length of 18 [8]. As the length of the battery string increases, the temperature of these batteries with negative voltage will be higher and higher. But the P-N junction has a maximum temperature, usually the current will be greatly increased and the device temperature is also rising rapidly when the silicon-based material PN junction over 150°C, which leads to irreversible damage of its function. In order to avoid this damage, we often use parallel bypass diode method or series isolation diode method and others. When a negative voltage of a battery reaches a certain level, the bypass diode can short-circuit the battery to protect itself or block the reverse current to protect the battery to work safely.

4. Composition and working characteristics of PV arrays

The PV array can be divided into S-structure, P-structure, SP-structure，TCT-structure and BL-structure, etc. The output characteristics of different structural arrays are also different.

4.1.Series structure (S structure)

The series(S) structure of the PV array is shown in Fig.3, assuming that the output voltage of one PV module is U_i, the output current is I_i, then the output voltage of the array is U and the output current is I. When the array is under normal working condition, according to the kirchhoff's law (KVL), the output characteristics of the array are shown in Eq. (11), and the output curve is similar to Fig.2.

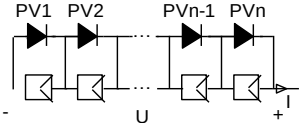

Fig.3 Series structure of PV arrays

$$\begin{cases} U = U_1 + U_2 + \ldots + U_n = \sum_{i=1}^{n} U_i \\ I = I_i \\ P = P_1 + P_2 + \ldots + P_n = \sum_{i=1}^{n} P_i \\ P_i = U_i \times I_i \end{cases} \quad (11)$$

The parameters I_i and U_i can be solved by Eq. (2) ~Eq. (7). When the PV array is in the case of partial shadows, the PV module under the shadow of the array may have a negative voltage due to non-uniform irradiation, and the PV module will work in the second quadrant. That is, the PV module is turned into a load state, and according to the reasons described in the previous section, there may be hot spots on the array at this time. However, the bypass diode of the PV cell will turn on to protect the battery. At this time the output current of each PV cell will also show the characteristics of the piecewise function, as shown in eq. (12)

$$\begin{cases} U = U_1 + \ldots U_{m-1} + U_{m+1} \ldots U_n = \sum_{i=1}^{n-1} U_i ; I_m < I < I_i \\ \cdots \\ U = U_1 + \ldots U_{n-m} = \sum_{i=1}^{n-m} U_i ; I_x < I_m < I < I_i \\ I = I_i ; I_i = I_{normal} \\ P = P_1 + P_2 + \ldots + P_n = \sum_{i=1}^{n-1} P_i \\ P_i = U_i \times I_i \end{cases} \tag{12}$$

Then the output characteristics of the array will also change, the output characteristics are shown in Fig. 4. Take four modules in series as an example, assuming the battery 1~4 received the light intensity distribution were shown in the table 1, the maximum power also shows in this Table.

Table 1 different irradiance (W/m^2) accepted by the series array & MPP (P/V)

1	2	3	4	Average value	MPP
1000	1000	1000	1000	1000	238.9W/67.569V
1000	900	800	700	850	183.1W/71.569V
300	500	700	900	600	97.32W/52.956V
740	480	350	670	560	93.27W/73..569V

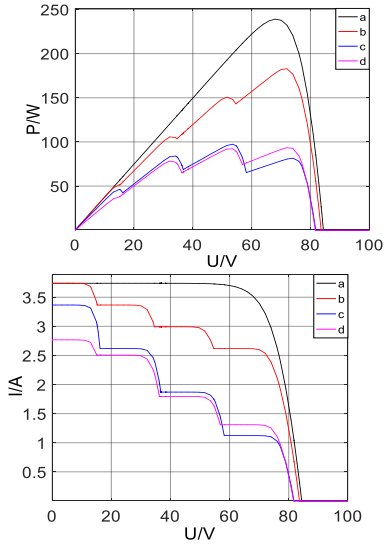

Fig.4 Output curve of Series array under different irradiance

4.2.Parallel structure (P structure)

The Parallel(P) structure of the PV array is shown in Fig.5.When the array is under normal working condition, according to the kirchhoff's law(KCL)，the output characteristics of the array are shown in Eq.(13), the output characteristics are similar to Fig.2.

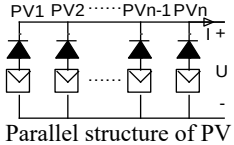

Fig.5 Parallel structure of PV arrays

$$\begin{cases} I = I_1 + I_2 + \cdots + I_n = \sum_{i=1}^{n} I_i \\ U = U_i \\ P = P_1 + P_2 + \cdots + P_n = \sum_{i=1}^{n} P_i \end{cases} \tag{13}$$

The parameters I_i and U_i can be solved by Eq. (2) ~ Eq. (7). When the PV array is in the case of partial shadows, due to the voltage of the PV module may be less than the output voltage of the array, the module under shadow will be protected due to the anti-backlash diode, but the energy of this module will be lost. The Eq. (14) can be obtained according to the Kirchhoff's law. Assume that four modules in parallel as an example, the irradiance parameters accepted are also shown in Table 1, the maximum power characteristics are shown in Table 2, the output characteristics are shown in Fig.6.

$$\begin{cases} I = I_1 + \ldots I_{m-1} + I_{m+1} \ldots I_n = \sum_{i=1}^{n-1} I_i ; I_m < I < I_i \\ \cdots \\ I = I_1 + \ldots I_{n-m} = \sum_{i=1}^{n-m} I_i ; I_x < I_m < I < I_i \\ U = U_i ; U_i = U_{normal} \\ P = P_1 + P_2 + \ldots + P_n = \sum_{i=1}^{n-1} P_i \\ P_i = U_i \times I_i \end{cases} \quad (14)$$

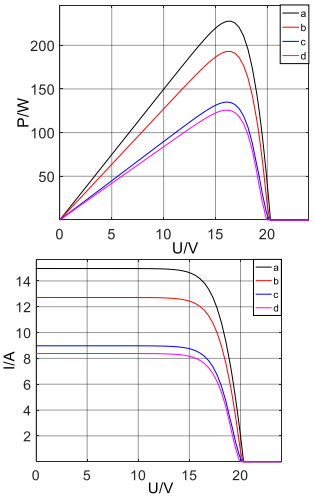

Fig.6 Output curve of Series array under different irradiance

Table 2 The MPP (P/V) of parallel array under different irradiance (W/m^2)

a	227.8W/16.457V	b	193.0W/16.457V
c	135.0W/16.038V	d	125.8W/16.038V

4.3.SP structure

The Series-Parallel structure shows in Fig.7, at this time the PV modules can be numbered of $PV_{m,n}$ in the matrix form because of the PV array presents matrix form. This structure is different form the above structure, there may be a negative voltage phenomenon occurs as in the series array, or there may be some substring voltage is too low and will cause current back-flush. So, the output of the substring need to be installed an anti-backlash diode to protect the substring. In the array of SP structures, the characteristics of the series substring conform to the characteristics of the S-array similar to Eq.(12), while the parallel characteristics of the array conform to the characteristics of the P-array similar to Eq.(14), the output characteristic of the SP structure is shown in Eq. (15).

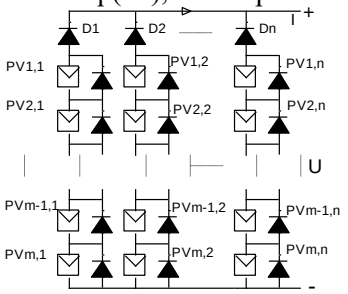

Fig.7 SP structure of PV arrays

$$\begin{cases} I = I_1 + I_2 \cdots + I_n = \sum_{i=1}^{n} I_i \\ U = U_1 + U_2 \cdots + U_m = \sum_{i=1}^{m} U_i \\ P = P_{1,1} + P_{2,1} + \cdots + P_{m,n} = \sum_{i=1}^{m \times n} P_{i,j} \end{cases} \quad (15)$$

Taking 4 × 3 PV array as an example, let the shadow distribution shown in Fig.8, assuming that the irradiance data is shown in Table 3, the output curve & characteristics are shown in Fig.9 & Table 3.

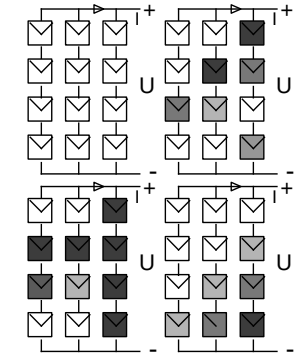

Fig.8 The distribution of shadows

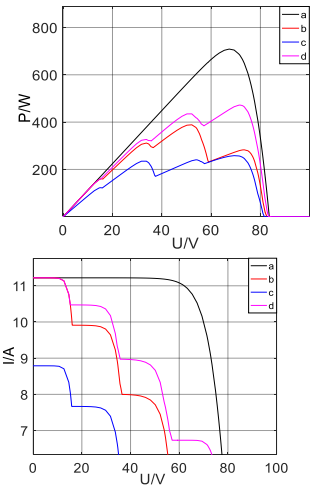

Fig.9 Output curve of the SP array in different shadows

Table 3 The different irradiance (W/m^2) accepted by the series array & MPP (P/V)

		1	2	3		1	2	3		1	2	3		1	2	3
1		100	100	100		100	100	350		100	100	35		100	100	100
2		100	100	100		100	300	440		350	350	35		100	100	800
3		100	100	100		400	700	100		470	700	35		100	800	600
4	a	100	100	100	b	100	100	650	c	100	100	35	d	800	600	400
Averag			1000				736.67				605.83				833.3	
MPP			708.8W/67.341V				389.3W/52.173V				295.1W/53.456V				470.8W/72.425V	

It can be seen from the experimental results that the output power curves in different shadows show the comprehensive characteristics of S-structure and P-structure, all of which have multi-peak and step-down characteristics. In addition, after several different shadow experiments, we can find that the maximum power point of the SP-structure is different with the distribution of the irradiance, and the maximum power point position is different.

4.4.TCT structure

The TCT-structure of the PV array is the Total-Cross-Tie structure of the PV modules, according to the number of diodes used in PV array that can be divided into several types shown in Fig.10.

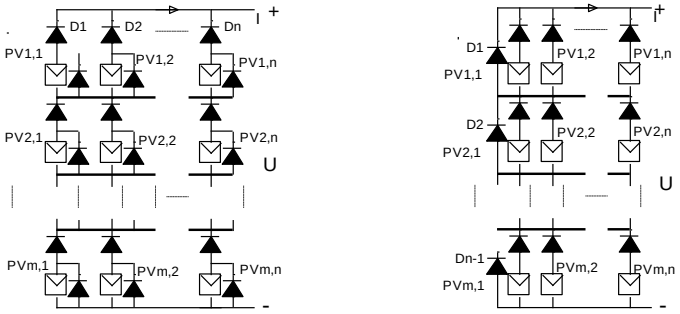

(a) Types of 2m×n (b) Types of (m+1)×n

Fig.10 TCT structure of PV arrays

The TCT structure of the PV array is based on the structure of the SP, then connected to the same line of the battery, and finally formed a parallel - series structure. The output current of the array is the sum of the currents of the parallel substrings, and the output voltage is the sum of the voltages of the series components. There may be many meshes or loops in this structure because of there are many

wires in the TCT array, however, when the array in different shadows, it is possible that the current anti-irrigation caused by the battery voltage in the array is not balanced, or the hot spot caused by the current imbalance. In this paper, we take two schemes as shown in Fig.10-a and Fig.10-b.The conduction condition of the bypass diode is similar to that of the S-structure, and the effect of the anti-backlash diode is similar to that of the P-structure. Similar to the previous structure, the parallel characteristics of the array conform to the characteristics of the P-array, and the series characteristics of the array conform to the characteristics of S- array. Similarly, the series characteristics in the TCT array conform to the characteristics similar to Eq. (12), the parallel characteristics conform to the characteristics similar to Eq. (14), the overall output characteristic expression of the SP structure array conforms to the characteristics similar to Eq. (15).

The output characteristic curve of TCT structure is also no longer similar as the curve in Fig.2. Similar to the previous section, the 4×3 TCT structure is taken as an example, assuming the shadow situation is consistent with Fig.8 , the irradiance parameters are same as the data in Table 3. The output MPP characteristics are shown in Table 4, the output curve of the two structural are similar, as shown in Fig.11, the output power is also closer, but the structure shown in 10-b saves m× (n-1) diodes.

Table 4 The MPP (P/V) of TCT array under different irradiance (W/m^2)

10-a	683.5W/65.133V	436.0W/67.727V
	278.9W/49.748V	461.0W/69.415V
10-b	683.6W/65.397V	437.0W/68.492V
	281.6W/50.371V	460.9W/70.192V

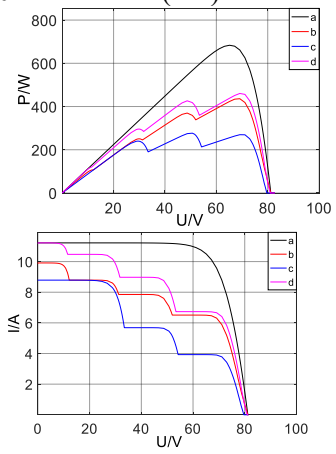

Fig.11 Output curve of the TCT array in different shadows

4.5.BL structure

The complexity of the bridge structure (BL) structure is between SP structure and TCT structure, and its structure is shown in Fig.12. From the Fig.12, we can see the BL structure reduces the number of wires on the basis of the TCT structure.

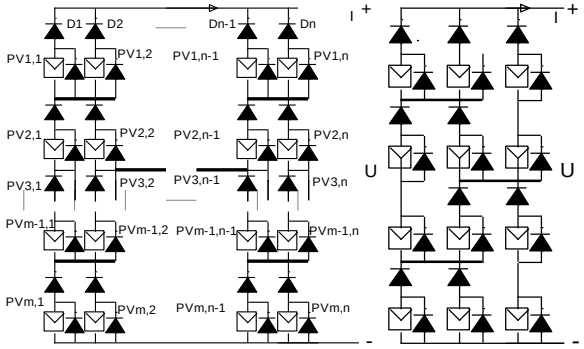

(a) BL structure schematic (b) 4 × 3 BL structure

Fig.12 BL structure of PV arrays

According to Kirchhoff's law (KVL, KCL) and the characteristics of the BL structure, it can be seen that the principle similar to that of SP&TCT array, the series characteristics in the BL array conform to the characteristics similar to Eq. (12), the parallel characteristics conform to the

characteristics similar to Eq. (14), the overall output characteristic expression of the SP structure array conforms to the characteristics similar to Eq.(15). As the BL structure reduces part of the wire, partial loop circuits can be reduced, so we can reduce part of diodes. Taking the 4 × 3 structure as an example, the simplified BL structure is shown in Fig.12-b, the turn-on condition of the bypass diode is similar to that in the S-array, and the protection of the anti-backlash diode is similar to that in the P-array. It is also assumed that the shadow situation is consistent with Fig.8, the irradiance parameters are same as the data in Table 3, the MPP characteristics are shown in Table 5, the output characteristics are shown in Fig.13.

Table 5 The MPP (P/V) of BL array under different irradiance (W/m^2)

a	683.2W/65.873V	b	409.4W/48.919V
c	273.7W/50.603V	d	460.4W/69.453V

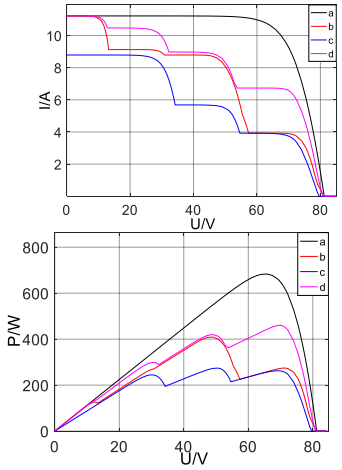

Fig.13 Output curve of the BL array in different shadows

4.6.Analysis and research on the characteristics of different structures

From the above simulation it can be seen that the mpp position of the array is different under different shadow, and sometimes the mpp position is at the right peak, while sometimes shifting to the left peak. From Table 1 ~ 2, we can see that the output power of the two arrays in different shades is different, and the output power of s-array in a slight shadow is greater than the P-array, but with the increase of the degree of shadows, the output power of S-array is gradually smaller than that of the P array. From Table 3 ~ 5, it can be seen that the three arrays also show similar changes in different shadows. After several simulation experiments it can be concluded that If the shadows are more average, the output power of the array TCT > BL > SP, But when there is a large gap between the irradiance received by each battery, the output power will be SP > BL > TCT. Because of the maximum power of SP, TCT and BL array is different， so it is possible to select the array structure with the largest power in work.

5. Conclusions

In this paper, the simulation experiment is carried out based on the mathematical model of PV cell. In addition, both different shadows and different array structures have an effect on the output characteristics of the PV array. Therefore, the mathematical analysis and model simulation of S, P, SP, TCT and BL arrays are carried out in this paper. It is concluded that the output power of the array S> P, TCT> BL> SP is obtained under the condition that the shadow degree is small and the distribution is relatively uniform, but when the degree of shadow is more serious, the output power of the array P> S, SP> BL> TCT is obtained. It is possible to select the most suitable array according to the different shadow conditions to improve the work efficiency.

Acknowledgement

This work was supported by the Science Foundation of Tibet Autonomous Region(2016ZR-15-8); the Youth Scientific Research Foundation of Tibet University(ZDPJZK1508) ;the innovation Support Program for Young Teachers of Universities in Tibet Autonomous Region(QCZ2016-26,QCZ2016-

08); the National Natural Science Foundation of China(NSFC)(61461047).

References

[1] Bangyin Liu, Shanxu Duan, Yong Kang. Modeling and analysis of characteristics PV module with partial Shading [J] . Acta Energiae Solaris Sinica, 2008, (02): 188-192.
[2] Ishaque K, Salam Z, Taheri H, et al. Modeling and simulation of photovoltaic (PV) system during partial shading based on a two-diode model[J]. Simulation Modelling Practice & Theory, 2011, 19(7):1613-1626.
[3] Wang Yanyun, Dongwei Xia. Modeling and series characteristics analysis of the PV array under partial shading conditions[J]. Electrical & Energy Management Technology, 2014, (15): 64-69.
[4] Fangfang Niu, Jianhui Su, Ailing Geng. Simplification of two-diode photovoltaic cell model [J]. Low Voltage Apparatus, 2012, (04): 27-30.
[5] Yunyun Wang. Effects of nonuniform temperature and irradiance on the photovoltaic performance of a PV/T system [D]. China University of Science and Technology, 2015.
[6] Skoplaki E, Palyvos J A. Operating temperature of photovoltaic modules: A survey of pertinent correlations[J].Renewable Energy, 2009, 34(1):23-29.
[7] Shanshou Li. Study on the analysis of mismatching and optimial control of PV system under shading conditions [D]. Hefei University of Technology, 2016.